Estimation of Laplacian Symbols for Analog Transmission over MIMO Channels

Author1, Author2 and Author3

***Abstract*—The MAP and MMSE estimation of Laplace-distributed symbols transmitted over Multiple Input Multiple Output channels is studied. This is an important problem in analog Joint Source Channel Coding with spiral mappings, where the probability density function of the transmitted symbols approximates a Laplace distribution in the low SNR regime. Simulation results are presented to illustrate the suitability of these estimators in uncoded and coded analog communications.**

***Keywords*—analog joint source channel coding, MMSE, MAP, estimation, MIMO.**

I. Introduction

ANALOG sources are often modeled as Gaussian random variables. When transmitting Gaussian symbols over communication channels with additive Gaussian noise, Linear Minimum Mean-Squared Error (LMMSE) estimation is the optimal receiving stategy provided the channel response is known [1]. LMMSE estimation is also helpful for the decoding of analog symbols compressed with spiral-like mappings [2, 3]. In such case, the use of a two-step receiver structure based on the concatenation of a LMMSE filter and a Maximum Likelihood (ML) decoder was shown to achieve near optimal-performance with a complexity lower than that of optimal Minimum Mean-Squared Error (MMSE) decoding [4].

The optimality of LMMSE filtering is supported by the assumption of Gaussian symbols. In a number of practical situations, however, analog symbols are better modeled as Laplacian random variables. This occurs in speech [5, 6] and image [7] transmission, or in analog Joint Source Channel Coding (JSCC) when spiral-like mappings are used for data compression [2, 3]. In this latter case, the encoded symbols have been observed to not strictly follow a Gaussian distribution and better match a Laplace distribution, specially for low Signal-to-Noise Ratio (SNR) values.

Parametric Maximum A Posteriori (MAP) and MMSE estimation with Laplacian prior has already been studied in the context of speech and image processing [5, 7, 8]. Furthermore, some feature selection techniques, such as the Lasso regression [9], can be interpreted as Bayesian MAP estimators under the assumption of Laplacian priors. In analog communications, the MMSE design criterion is a suitable one since it minimizes analog symbol distortion which is typically measured as the Mean-Squared Error (MSE) between transmitted and received symbols. In this work, we consider the MMSE estimation of Laplace-distributed symbols transmitted over fading Multiple-Input Multiple-Output (MIMO) channels, following the classical Bayesian approach. The effect of the MIMO fading channel is incorporated in the estimator derivation to obtain more general expressions than previous works focused on SISO transmissions over AWGN channels. This estimator is evaluated for analog JSCC transmissions, showing its suitability for the transmission of compressed uncorrelated Gaussian sources. Additionally, its performance is compared to that obtained with MAP, LMMSE and to the optimal cost-distortion tradeoff.

The rest of the paper is organized as follows. Section II describes the system model considered along this work. Sections III and IV focus on the MAP and MMSE estimation of symbols transmitted over Rayleigh MIMO channels with Laplace prior. Section V evaluates the performance of the MAP and MMSE estimators via computer simulations. Finally, section VI is devoted to the conclusions.

II. System Model

Let us consider a discrete-time analog MIMO communication system where a set of complex-valued continuous-amplitude symbols $\{x_n\}_{n=1}^{n_T}$ are transmitted over a MIMO channel with n_T transmit and n_R receive antennas. We assume channel symbols are Laplace-distributed with unit variance, and independent and identically distributed (i.i.d.) real and imaginary parts, i.e. $\Re\{x_n\}, \Im\{x_n\} \sim \mathcal{L}(0,1)$. Let us stack these symbols in the following $2n_T \times 1$ vector

$$\mathbf{x} = [\Re\{x_1\}, \Im\{x_1\}, \ldots, \Re\{x_{n_T}\}, \Im\{x_{n_T}\}]^T, \tag{1}$$

whose probability density function (pdf) is given by

$$p(\mathbf{x}) = \exp\left(-2|\mathbf{x}|\right) = \exp\left(-2\mathrm{sgn}(\mathbf{x})^T\mathbf{x}\right), \tag{2}$$

where $|\cdot|$ is the norm-1 operator, and $\mathrm{sgn}(\mathbf{x}) = [\mathrm{sgn}([\mathbf{x}]_1), \ldots, \mathrm{sgn}([\mathbf{x}]_{2n_T})]^T$ is the sign operator.

We now represent the MIMO channel output symbols as

$$\mathbf{y} = \mathbf{H}\mathbf{x} + \mathbf{w}, \tag{3}$$

where $\mathbf{H} \in \mathbb{R}^{2n_R \times 2n_T}$ is the real-valued channel response matrix

$$\mathbf{H} = \begin{pmatrix} \mathbf{H}_{1,1} & \mathbf{H}_{1,2} & \cdots & \mathbf{H}_{1,n_T} \\ \mathbf{H}_{2,1} & \mathbf{H}_{2,2} & \cdots & \mathbf{H}_{2,n_T} \\ \cdots & \cdots & \cdots & \cdots \\ \mathbf{H}_{n_R,1} & \mathbf{H}_{n_R,2} & \cdots & \mathbf{H}_{n_R,n_T} \end{pmatrix}, \tag{4}$$

with the 2×2 matrices

$$\mathbf{H}_{i,j} = \begin{pmatrix} \Re\{h_{i,j}\} & -\Im\{h_{i,j}\} \\ \Im\{h_{i,j}\} & \Re\{h_{i,j}\} \end{pmatrix} \quad \begin{matrix} i = 1, \ldots, n_R \\ j = 1, \ldots, n_T \end{matrix} \tag{5}$$

determined by the real and imaginary parts of the channel response $h_{i,j}$, between the j-th transmit antenna an the i-th receive antenna. The additive Gaussian noise is given by

$$\mathbf{w} = [\Re\{w_1\}, \Im\{w_1\}, \ldots, \Re\{w_{n_R}\}, \Im\{w_{n_R}\}]^T, \tag{6}$$

where $\{w_n\}_{n=1}^{n_R}$ are the complex-valued noise components with $w_n \sim \mathcal{CN}(0, \sigma_w^2)$. The noise is assumed to be spatially white. Hence, $\mathbf{w} \sim \mathcal{N}(\mathbf{0}, \frac{\sigma_w^2}{2}\mathbf{I}_{2n_R})$. According to this signal model, the conditional pdf of the received signal is

$$p(\mathbf{y}|\mathbf{x}) = \frac{1}{\pi^{n_R}\sigma_w^{2n_R}} \exp\left(-\frac{\|\mathbf{y}-\mathbf{H}\mathbf{x}\|^2}{\sigma_w^2}\right). \quad (7)$$

III. MAP ESTIMATOR

For a given $\mathbf{y}$, the MAP estimate of $\mathbf{x}$ is

$$\hat{\mathbf{x}}_{\text{MAP}} = \arg\max_{\mathbf{x}} \; p(\mathbf{x}|\mathbf{y}), \quad (8)$$

where $p(\mathbf{x}|\mathbf{y})$ is the *a posteriori* pdf of $\mathbf{x}$. Applying Bayes rule, such pdf is rewritten as

$$p(\mathbf{x}|\mathbf{y}) = \frac{p(\mathbf{y}|\mathbf{x})p(\mathbf{x})}{p(\mathbf{y})}. \quad (9)$$

We now denote $g(\mathbf{x}) = \ln(p(\mathbf{x}|\mathbf{y}))$

$$g(\mathbf{x}) = \ln\left(\frac{1}{\sqrt{\pi\sigma_w^2}}\right) - \frac{\|\mathbf{y}-\mathbf{H}\mathbf{x}\|^2}{\sigma_w^2} - 2|\mathbf{x}| - \ln(p(\mathbf{y})). \quad (10)$$

Hence, the MAP estimation problem can be formulated as

$$\hat{\mathbf{x}}_{\text{MAP}} = \arg\min_{\mathbf{x}} \quad \|\mathbf{y}-\mathbf{H}\mathbf{x}\|^2 + 2\sigma_w^2|\mathbf{x}|. \quad (11)$$

This problem has already been studied in the literature, in particular in image and voice processing [7, 8]. Given that this cost function is non-differentiable, different approaches have been studied to solve it, such as steepest descent search or iterative-shrinkage algorithms [7]. However, this problem simplifies if $\mathbf{H}^T\mathbf{H}$ is diagonal, in which case the MAP estimate can be written as

$$\hat{\mathbf{x}}_{\text{MAP}} = \mathbf{A}\left(\mathbf{A}\hat{\mathbf{x}}_{\text{LS}} - \sigma_w^2(\mathbf{H}^T\mathbf{H})^{-1}\mathbf{1}\right)^+. \quad (12)$$

with $(\cdot)^+ = \max[0,\cdot]$ and $\mathbf{A} = \text{diag}\{\text{sgn}(\hat{\mathbf{x}}_{\text{LS}})\}$ a $2n_T \times 2n_T$ matrix that multiplied by $\hat{\mathbf{x}}_{\text{LS}}$ allows to first compute the absolute value of each component and then restore the original sign. The proof for (12) is analogous to the one described in [8] when $\mathbf{H}$ is unitary.

IV. MMSE ESTIMATOR

For a given $\mathbf{y}$, the MMSE estimate of $\mathbf{x}$ is

$$\hat{\mathbf{x}}_{\text{MMSE}} = E(\mathbf{x}|\mathbf{y}) = \int \mathbf{x}p(\mathbf{x}|\mathbf{y})d\mathbf{x} = \frac{\int \mathbf{x}p(\mathbf{y}|\mathbf{x})p(\mathbf{x})d\mathbf{x}}{\int p(\mathbf{y}|\mathbf{x})p(\mathbf{x})d\mathbf{x}}. \quad (13)$$

Substituting (7) and (2) into (13) yields

$$\hat{\mathbf{x}}_{\text{MMSE}} = \frac{\int \mathbf{x}\exp\left(-\sigma_w^{-2}\|\mathbf{y}-\mathbf{H}\mathbf{x}\|^2 - 2\text{sgn}(\mathbf{x})^T\mathbf{x}\right)d\mathbf{x}}{\int \exp\left(-\sigma_w^{-2}\|\mathbf{y}-\mathbf{H}\mathbf{x}\|^2 - 2\text{sgn}(\mathbf{x})^T\mathbf{x}\right)d\mathbf{x}}. \quad (14)$$

We now split the integrals in (14) into a sum of individual integrals for each orthant $\mathcal{O}_i$, and (14) can be rewritten as

$$\hat{\mathbf{x}}_{\text{MMSE}} = \frac{\sum_i \int_{\mathbf{a}_i}^{\mathbf{b}_i} \mathbf{x}\exp\left(-\sigma_w^{-2}\|\mathbf{y}-\mathbf{H}\mathbf{x}\|^2 - 2\boldsymbol{\delta}_i^T\mathbf{x}\right)d\mathbf{x}}{\sum_i \int_{\mathbf{a}_i}^{\mathbf{b}_i} \exp\left(-\sigma_w^{-2}\|\mathbf{y}-\mathbf{H}\mathbf{x}\|^2 - 2\boldsymbol{\delta}_i^T\mathbf{x}\right)d\mathbf{x}}, \quad (15)$$

with the following integral limits

$$[\mathbf{a}_i]_j = \begin{cases} -\infty & [\boldsymbol{\delta}_i]_j = -1 \\ 0 & [\boldsymbol{\delta}_i]_j = 1 \end{cases}$$
$$[\mathbf{b}_i]_j = \begin{cases} 0 & [\boldsymbol{\delta}_i]_j = -1 \\ \infty & [\boldsymbol{\delta}_i]_j = 1. \end{cases}$$

We now elaborate Eq. (15) as

$$\hat{\mathbf{x}}_{\text{MMSE}} = \frac{\sum_i \int_{\mathbf{a}_i}^{\mathbf{b}_i} \mathbf{x}\exp\left(-\sigma_w^{-2}\mathbf{x}^T\mathbf{H}^T\mathbf{H}\mathbf{x} + 2(\sigma_w^{-2}\mathbf{y}^T\mathbf{H} - \boldsymbol{\delta}_i^T)\mathbf{x}\right)d\mathbf{x}}{\sum_i \int_{\mathbf{a}_i}^{\mathbf{b}_i} \exp\left(-\sigma_w^{-2}\mathbf{x}^T\mathbf{H}^T\mathbf{H}\mathbf{x} + 2(\sigma_w^{-2}\mathbf{y}^T\mathbf{H} - \boldsymbol{\delta}_i^T)\mathbf{x}\right)d\mathbf{x}}. \quad (16)$$

Introducing $\boldsymbol{\mu}_i = \hat{\mathbf{x}}_{\text{LS}} - \sigma_w^2(\mathbf{H}^T\mathbf{H})^{-1}\boldsymbol{\delta}_i$ and $\mathbf{C} = \sigma_w^2(\mathbf{H}^T\mathbf{H})^{-1}$, (16) is rewritten as

$$\begin{aligned}\hat{\mathbf{x}}_{\text{MMSE}} &= \frac{\sum_i \exp(\boldsymbol{\mu}_i^T\mathbf{C}^{-1}\boldsymbol{\mu}_i)\int_{\mathbf{a}_i}^{\mathbf{b}_i}\mathbf{x}\exp(-(\mathbf{x}-\boldsymbol{\mu}_i)^T\mathbf{C}^{-1}(\mathbf{x}-\boldsymbol{\mu}_i))d\mathbf{x}}{\sum_i \exp(\boldsymbol{\mu}_i^T\mathbf{C}^{-1}\boldsymbol{\mu}_i)\int_{\mathbf{a}_i}^{\mathbf{b}_i}\exp(-(\mathbf{x}-\boldsymbol{\mu}_i)^T\mathbf{C}^{-1}(\mathbf{x}-\boldsymbol{\mu}_i))d\mathbf{x}} \\ &= \frac{\sum_i \exp(\boldsymbol{\mu}_i^T\mathbf{C}^{-1}\boldsymbol{\mu}_i)\int_{\mathbf{a}_i-\boldsymbol{\mu}_i}^{\mathbf{b}_i-\boldsymbol{\mu}_i}(\mathbf{x}+\boldsymbol{\mu}_i)\exp(-\mathbf{x}^T\mathbf{C}^{-1}\mathbf{x})d\mathbf{x}}{\sum_i \exp(\boldsymbol{\mu}_i^T\mathbf{C}^{-1}\boldsymbol{\mu}_i)\int_{\mathbf{a}_i-\boldsymbol{\mu}_i}^{\mathbf{b}_i-\boldsymbol{\mu}_i}\exp(-\mathbf{x}^T\mathbf{C}^{-1}\mathbf{x})d\mathbf{x}}. \end{aligned} \quad (17)$$

Denoting $\phi_i = \exp(\boldsymbol{\mu}_i^T\mathbf{C}^{-1}\boldsymbol{\mu}_i)\int_{\mathbf{a}_i-\boldsymbol{\mu}_i}^{\mathbf{b}_i-\boldsymbol{\mu}_i}\exp(-\mathbf{x}^T\mathbf{C}^{-1}\mathbf{x})d\mathbf{x}$, and $\boldsymbol{\zeta}_i = \exp(\boldsymbol{\mu}_i^T\mathbf{C}^{-1}\boldsymbol{\mu}_i)\int_{\mathbf{a}_i-\boldsymbol{\mu}_i}^{\mathbf{b}_i-\boldsymbol{\mu}_i}\mathbf{x}\exp(-\mathbf{x}^T\mathbf{C}^{-1}\mathbf{x})d\mathbf{x}$, and replacing $\boldsymbol{\mu}_i$ by its definition, we obtain

$$\begin{aligned}\hat{\mathbf{x}}_{\text{MMSE}} &= \frac{\sum_i(\boldsymbol{\mu}_i\phi_i + \boldsymbol{\zeta}_i)}{\sum_i \phi_i} \\ &= \hat{\mathbf{x}}_{\text{LS}} - \sigma_w^2(\mathbf{H}^T\mathbf{H})^{-1}\frac{\sum_i \boldsymbol{\delta}_i\phi_i}{\sum_i\phi_i} + \frac{\sum_i\boldsymbol{\zeta}_i}{\sum_i\phi_i}. \end{aligned} \quad (18)$$

Observe that if $\mathbf{C}$ is diagonal, the calculation of (18) significantly simplifies. Indeed, denoting $\rho_j = [\mathbf{C}]_{j,j}$ as the j-th diagonal entry of $\mathbf{C}$, $\mu_j^+ = [\hat{\mathbf{x}}_{\text{LS}}]_j + \rho_j$, and $\mu_j^- = [\hat{\mathbf{x}}_{\text{LS}}]_j - \rho_j$, it can be shown that $\sum_i \boldsymbol{\zeta}_i = 0$, and also that

$$\sum_i [\boldsymbol{\delta}_i]_j\phi_i = \frac{\pi}{2}\left(\text{erfcx}(-\mu_j^-/\sqrt{\rho_j}) - \text{erfcx}(\mu_j^+/\sqrt{\rho_j})\right) \times \prod_{k\neq j}^{2n_T}\frac{\pi}{2}\left(\text{erfcx}(-\mu_k^-/\sqrt{\rho_k}) + \text{erfcx}(\mu_k^+/\sqrt{\rho_k})\right) \quad (19)$$

$$\sum_i \phi_i = \prod_{j=1}^{2n_T}\frac{\pi}{2}\left(\text{erfcx}(-\mu_j^-/\sqrt{\rho_j}) + \text{erfcx}(\mu_j^+/\sqrt{\rho_j})\right), \quad (20)$$

where $\text{erfc}(x) = \frac{2}{\pi}\int_x^\infty \exp(-t^2)dt$ is the complementary error function and $\text{erfcx}(x) = \exp(x^2)\text{erfc}(x)$. Substituting (19) and

(20) into (18), yields the following expression for $\hat{\mathbf{x}}_{\text{MMSE}}$ when $\mathbf{C}$ is diagonal

$$\hat{\mathbf{x}}_{\text{MMSE}} = \hat{\mathbf{x}}_{\text{LS}} - \sigma_w^2(\mathbf{H}^T\mathbf{H})^{-1}\boldsymbol{\theta}, \tag{21}$$

where $\boldsymbol{\theta}$ is a vector whose i-th entry is given by

$$[\boldsymbol{\theta}]_i = \frac{\text{erfcx}\left(\frac{-\mu_i^-}{\sqrt{\rho_i}}\right) - \text{erfcx}\left(\frac{\mu_i^+}{\sqrt{\rho_i}}\right)}{\text{erfcx}\left(\frac{-\mu_i^-}{\sqrt{\rho_i}}\right) + \text{erfcx}\left(\frac{\mu_i^+}{\sqrt{\rho_i}}\right)}. \tag{22}$$

A. Remarks

1) The general MMSE expression in (18) requires the computation of orthant cumulative distribution functions of multivariate Gaussians in the ϕ_i terms. As shown in [10], low complexity approximations are only known for distributions up to three variables. For higher dimensions, other techniques such as the Monte Carlo methods can be used, which have a large computational complexity as long as the number of dimensions grows.
2) The MAP and MMSE estimates when $\mathbf{C}$ is diagonal converge to the same form when the components of $\hat{\mathbf{x}}_{\text{LS}}$ are large enough. In that case $\boldsymbol{\theta}$ equals to $\text{sgn}(\hat{\mathbf{x}}_{\text{LS}})$.
3) The MMSE estimate in (21) is similar to the one defined in [5], although (21) incorporates the effect of the MIMO channel coefficients.
4) The LMMSE estimator is given by

$$\hat{\mathbf{x}}_{\text{LMMSE}} = (\mathbf{H}^T\mathbf{H} + \sigma_w^2\mathbf{I}_{2n_T})^{-1}\mathbf{H}^T\mathbf{y}. \tag{23}$$

The computational complexity of the LMMSE and MMSE estimates is similar when $\mathbf{C}$ is diagonal. Indeed, the complexity of the LMMSE estimate is mainly determined by the inversion of a diagonal matrix, which is linear, whereas the MMSE estimate depends on the element-wise computation of $\boldsymbol{\theta}$, which is also linear.
5) Expressions (12) and (21) significantly simplify for a SISO system. In such case, $\sigma_w^2(\mathbf{H}^T\mathbf{H})^{-1} = \frac{\sigma_w^2}{\|h\|^2}\mathbf{I}_2$ where h is the complex-valued SISO channel response.

V. Simulation Results

In this section the results of several computer experiments are presented to illustrate the performance of the MAP and MMSE estimators derived in the previous sections. We consider spatially white Rayleigh 4×4 MIMO channels, i.e. channel entries are i.i.d. complex-valued zero-mean circularly symmetric Gaussian random variables. Let us consider the Singular Value Decomposition (SVD) of the MIMO channel matrix $\mathbf{H} = \mathbf{U}\boldsymbol{\Sigma}\mathbf{V}^H$ where $\mathbf{U}$ and $\mathbf{V}$ are unitary matrices and $\boldsymbol{\Sigma}$ is a diagonal matrix. If the input $\mathbf{x}$ is the result of precoding $\tilde{\mathbf{x}}$ with $\mathbf{V}$ (i.e. $\mathbf{x} = \mathbf{V}\tilde{\mathbf{x}}$) the MIMO channel output is

$$\mathbf{y} = \mathbf{H}\mathbf{V}\tilde{\mathbf{x}} + \mathbf{w} = \mathbf{U}\boldsymbol{\Sigma}\tilde{\mathbf{x}} + \mathbf{w} = \tilde{\mathbf{H}}\tilde{\mathbf{x}} + \mathbf{w}. \tag{24}$$

The equivalent MIMO channel response matrix $\tilde{\mathbf{H}} = \mathbf{U}\boldsymbol{\Sigma}$ enables the use of the simplified expressions for the MAP and MMSE estimators, since $\tilde{\mathbf{H}}^T\tilde{\mathbf{H}}$ is diagonal.

Two different scenarios are considered: uncoded transmission of Laplace-distributed source symbols and 2:1 compression of Gaussian sources using analog JSCC with spiral mappings. In the latter case, the transmitted symbols are generated as $\tilde{\mathbf{x}} = \text{g}(\mathbf{s}_1, \mathbf{s}_2)$, where $\mathbf{s}_1$ and $\mathbf{s}_2$ are the source symbols, and $\text{g}(\cdot)$ is the joint source-channel encoder. At the receiver an estimate of the source symbols is obtained as $[\hat{\mathbf{s}}_1, \hat{\mathbf{s}}_2] = \text{h}(\hat{\mathbf{x}})$, where the decoder $\text{h}(\cdot)$ follows an ML approach [4]. The statistical distribution of the analog JSCC symbols $\tilde{\mathbf{x}}$ to be transmitted depends on the source symbols distribution and the particular shape of the Archimedean spiral employed at the encoding step. Previous work [11] suggests that the performance of analog JSCC systems is improved if the encoder $\text{g}(\cdot)$ is specifically optimized for each channel SNR value. When empirically analyzing the distribution of the analog encoded symbols in such situation, we observe that this distribution is more like a Laplacian than a Gaussian for low and medium SNRs. This can be measured by means of the Jensen-Shannon Divergence (JSD) given by

$$\begin{aligned}\text{JSD}(p,q) =& \frac{1}{2}\int_{-\infty}^{\infty} p(x)\ln\left(\frac{p(x)}{q(x)}\right)\text{d}x \\ &+\frac{1}{2}\int_{-\infty}^{\infty} q(x)\ln\left(\frac{q(x)}{p(x)}\right)\text{d}x,\end{aligned} \tag{25}$$

where $p(x)$ and $q(x)$ are the pdfs to be compared. Figure 1 plots the JSD between the distribution of the analog JSCC symbols and the Gaussian and Laplacian distributions for a range of SNRs between 0 and 30 dB. It is apparent from this figure that the distribution of the analog encoded symbols is more like a Laplacian for SNRs below 16 dB while this behavior reverses for higher SNRs. Remark that the distribution of the encoded symbols and, therefore, the corresponding JSD values explicitly depend on the parameters of the non-linear mapping $\text{g}(\cdot)$, which is specifically optimized for each SNR. This analysis illustrates the suitability of the MAP and MMSE estimators derived in this paper for analog JSCC transmissions that use Archimedean spiral non-linear mappings.

The performance of analog communications is usually measured in terms of the Signal-to-Distortion Rate (SDR) with respect to the channel SNR. The SDR in dB is calculated as $\text{SDR} = 10\log_{10}\left(\sigma_s^2/D\right)$, where σ_s^2 is the source variance and $D = \frac{1}{N}\sum_{i=1}^{N}\text{E}\{\|\mathbf{s}_i - \hat{\mathbf{s}}_i\|^2\}$ is the observed MSE distortion, with N the source bandwidth, i.e. $N = 1$ in the case of uncoded Laplacian input and $N = 2$ for 2:1 encoded Gaussian inputs. The performance is upper bounded by the optimal cost-distortion tradeoff which is referred to as the Optimum Performance Theoretically Attainable (OPTA) in the literature. The OPTA is calculated by equating the source rate distortion function and the channel capacity, i.e.,$NR(D) = KC(\mathbf{H})$, where K is the channel bandwidth ($K = 1$ in this case), $C(\mathbf{H})$ is the channel capacity and $R(D)$ is the rate distortion function of the source. Note that the OPTA is difficult to determine when considering Laplacian input symbols because there are no closed-form expressions for $C(\mathbf{H})$ and $R(D)$. We circumvent this limitation by using the $C(\mathbf{H})$ expression for Gaussian inputs, and an upper bound for $R(D)$ in the case of Laplace-distributed sources [12].

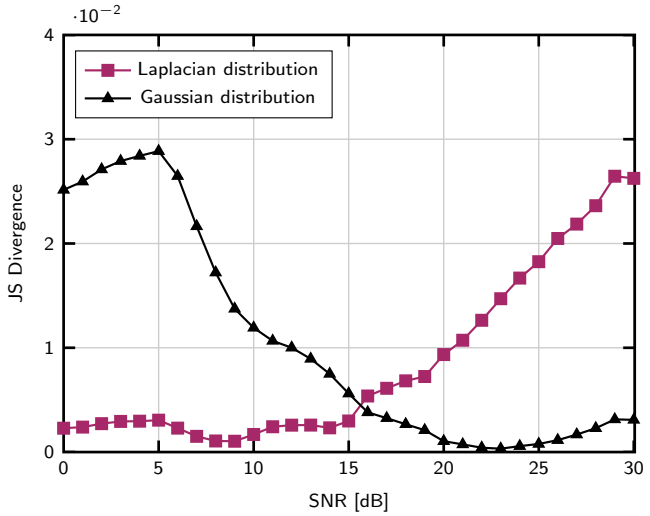

Fig. 1. Jensen-Shannon divergence of the analog JSCC encoder output.

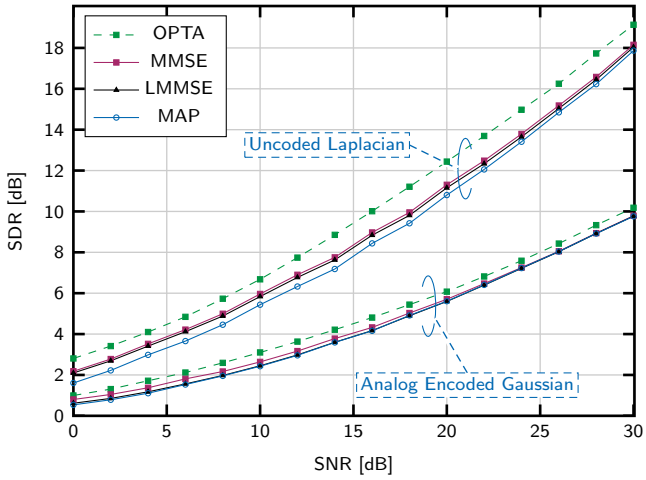

Fig. 2. Performance for uncoded Laplacian sources and 2:1 analog encoded Gaussian inputs. A spatially white Rayleigh 4×4 MIMO channel is assumed.

Figure 2 plots the performance obtained with the MAP and MMSE estimators for Laplace-distributed prior in the two considered scenarios. The performance obtained with LMMSE estimation and the OPTA is also included. As expected, a performance gain with respect to LMMSE is obtained when the MMSE estimator is used. This is because LMMSE is actually suboptimal when MIMO channel inputs are Laplace-distributed. However, the behaviour of both estimators is slightly different for each scenario. The gap between MMSE and LMMSE is always present for uncoded Laplacian symbols, while for 2:1 compressed Gaussian inputs, this gap is larger for low SNRs but vanishes for SNR values above 15 dB. These results show that the Laplacian MMSE estimation of the analog JSCC symbols improves the global system performance when channel inputs better match the Laplace distribution (see Figure 1). In any case, note from Figure 2 the good performance obtained with LMMSE estimation, in spite of the channel input symbols are sometimes not strictly Gaussian-distributed. LMMSE filtering hence provides a good tradeoff between complexity and performance at all ranges of SNRs.

On the other hand, the MAP estimator performs worse than MMSE and LMMSE in both cases. This is because the MAP estimator searches for the maximum of the a-posteriori probability, and does not minimize the MSE.

Finally, the system performance in the encoded case closely approaches the OPTA, while the gap to the OPTA is larger when considering uncoded Laplacian symbols. This is partially caused by the approximations in the OPTA calculation.

VI. Conclusions

In this work we have derived two suitable estimators for the transmission of Laplacian sources over MIMO channels: MAP and MMSE, which can be obtained by means of a subgradient approach, and by the numerical computation of complex integrals, respectively. These computations can be significantly simplified for precoded MIMO channels. The obtained results show the adequate performance of the MAP and the non-linear MMSE estimators. Nevertheless, such performance is close to that obtained with LMMSE, specially when considering the analog JSCC encoding of Gaussian sources with spiral mappings in the high SNR regime, where the Laplace distribution assumption is weaker.

References

[1] S. M. Kay, *Fundamentals of Statistical Signal Processing*. Prentice Hall, 1993.

[2] T. A. Ramstad, "Shannon mappings for robust communication," *Telektronikk*, vol. 98, no. 1, pp. 114–128, 2002.

[3] F. Hekland, P. Floor, and T. A. Ramstad, "Shannon-Kotel'nikov Mappings in Joint Source-Channel Coding," *IEEE Trans. Commun.*, vol. 57, no. 1, pp. 94–105, Jan 2009.

[4] O. Fresnedo, F. Vázquez-Araújo, L. Castedo, and J. García-Frías, "Low-Complexity Near-Optimal Decoding for Analog Joint Source Channel Coding Using Space-Filling Curves," *IEEE Commun. Lett.*, vol. 17, no. 4, pp. 745–748, Apr 2013.

[5] R. Martin and C. Breithaupt, "Speech Enhancement in the DFT Domain using Laplacian Speech Priors," in *Proc. International Workshop on Acoustic Echo and Noise Control (IWAENC 03*, 2003, p. 8790.

[6] B. Chen and P. C. Loizou, "A Laplacian-based MMSE estimator for speech enhancement," *Speech Communication*, vol. 49, no. 2, pp. 134 – 143, 2007.

[7] P. Moulin and J. Liu, "Analysis of multiresolution image denoising schemes using generalized Gaussian and complexity priors," *IEEE Trans. Inf. Theory*, vol. 45, no. 3, pp. 909–919, Apr 1999.

[8] M. Zibulevsky and M. Elad, "L1-L2 Optimization in Signal and Image Processing," *IEEE Signal Processing Magazine*, vol. 27, no. 3, pp. 76–88, May 2010.

[9] R. Tibshirani, "Regression Shrinkage and Selection via the Lasso," *Journal of the Royal Statistical Society. Series B (Methodological)*, vol. 58, no. 1, pp. pp. 267–288, 1996.

[10] A. Genz and F. Bretz, *Computation of Multivariate Normal and t Probabilities*, ser. Lecture Notes in Statistics. Springer Berlin Heidelberg, 2009.

[11] Y. Hu, J. García-Frías, and M. Lamarca, "Analog Joint Source-Channel Coding Using Non-Linear Curves and MMSE Decoding," *IEEE Trans. Commun.*, vol. 59, no. 11, pp. 3016–3026, Nov 2011.

[12] O. Fresnedo, "Analog Joint Source Channel Coding for Wireless Communications," Ph.D. dissertation, University of A Coruña, 2014.